Polymer Journal (2019) 51:1055–1061
https://doi.org/10.1038/s41428-019-0216-1

ORIGINAL ARTICLE

Synthesis of network polymer emitters: tunable detection of chemicals by geometric design

Shotaro Hayashi[1] · Shin-ichi Yamamoto[1] · Koji Nishi[1] · Atsushi Asano[1] · Toshio Koizumi[1]

Received: 20 March 2019 / Revised: 16 May 2019 / Accepted: 17 May 2019 / Published online: 7 June 2019

Abstract

Conjugated network polymer emitters are potential materials for use as solid detectors of chemicals. We demonstrated the synthesis of fluorescent network polymers through a facile route. Solid-state fluorescent network polymer emitters were synthesized through the Knoevenagel polycondensation of an arylaldehyde (tris(*p*-formylphenyl)amine) with an arylacetonitrile (phenylenediacetonitrile) in good yields. The molecular structure based on the electron-donor triphenylamine and electron-acceptor cyano-substituted phenylene-vinylene showed a highly efficient solid-state fluorescence. The synthesized model small molecule showed a well-defined solvatofluorochromism: the dielectric constants were ε_{sol} of approximately 0–50 at λ_{fl} of 480–560 nm. The response to solvent chemicals was also shown for the network polymers. Surprisingly, the network polymer linked with *para*-phenylene-vinylene was only responsive to the solvents with a low dielectric constant (ε_{sol} ca. <8) and nitrobenzene, for which ε_{sol} is approximately 35. This solvatofluorochromic behavior differed from that of the model compound. More interestingly, the network polymer linked with *meta*-phenylene-vinylene was responsive to the aromatic solvents only. Consequently, the characteristic chemoselectivity was observed by the geometric effect of the network structure.

Introduction

Since network polymers having microporous structures are of interest in reports on tunable pore sizes [1, 2], structural modularity [3], high surface areas [4, 5], and exceptional physicochemical stability [4], new materials have been developed for applications such as catalysis [6–8], light harvesting [9], carbon dioxide capture [10], superhydrophobic separations [11], luminescence [12], sensors [13], and supercapacitors [14]. Unlike crystalline network polymers, such as covalent organic frameworks [15, 16], organometallics (e.g., metal–organic frameworks) [17, 18], and inorganic materials (e.g., zeolites) [19, 20], the polymers are almost amorphous. The light-absorption and emission behaviors of conjugated structures in such materials are directly useful for said applications (especially as photocatalysts and sensors). Conjugated microporous polymers (CMPs) [21–23], which have been synthesized by carbon–carbon coupling chemistry [24–34], are able to yield insoluble polymer networks, and the insolubility offers the advantages of easy recovery and conventional purification.

Carbon–carbon coupling chemistry is a great advance in the synthesis of CMPs [24–34]. Recently, Pd-catalyzed cross-coupling (Suzuki [26], Heck [27], and Sonogashira [28]) CMP syntheses have been developed to construct networks with alternating structures of two or more aromatic units. More recently, the Pd-catalyzed direct C-H arylation reaction has also been shown to be a strong synthetic tool for network structure synthesis [29–31]. However, the methodology of metal-catalyst-free cross-coupling reactions is important for future CMP synthetic methods. The Knoevenagel condensation, the reaction of a ketone with a carbon nucleophile [32–34], is often an easily implemented and excellent tool for conjugated polymer synthesis owing to the metal-catalyst-free dehydration condensation. Only a few reports have focused on the synthesis of network polymers through such a

Supplementary information The online version of this article (https://doi.org/10.1038/s41428-019-0216-1) contains supplementary material, which is available to authorized users.

✉ Shotaro Hayashi
shayashi@nda.ac.jp

[1] Department of Applied Chemistry, National Defense Academy, 1-10-20, Hashirimizu, Yokosuka, Kanagawa 239-8686, Japan

polycondensation [35]. The polycondensation of arylaldehydes with arylacetonitrile gave cyano-substituted polyarylene-vinylene structures. The molecules that include such structures are known to exhibit solid-state fluorescence [32–34]. To advance polymers based on cyano-substituted polyarylene-vinylene, we conceived a tunable fluorescence by the geometric design of network structures. We report here the synthesis of network polymers through the Knoevenagel polycondensation and their solvent-sensing ability based on geometry-triggered chemoselectivity.

Materials and methods

Materials

Phenylacetonitrile (Sigma-Aldrich Co., LLC), *p*-xylene dicyanide (Tokyo Chemical Industry Co., Ltd: TCI), *m*-xylene dicyanide (TCI), *o*-xylene dicyanide, tris(*p*-formylphenyl)amine (TCI), and 1 M sodium methoxide in methanol (FUJIFILM Wako Pure Chemical Corporation) were used as received. All solvents were used after distillation.

Synthesis of 3

To a mixture of phenylacetonitrile (586 mg, 5.0 mmol) and tris(*p*-formylphenyl)amine (329 mg, 1.0 mmol) in ethanol (10 mL), sodium methoxide in methanol (1 M, 5 mL) was added and stirred for 10 min at room temperature under air. The reaction mixture was diluted with ethanol (10 mL) and then filtered to remove a solid. The solid was washed with ethanol (10 mL) and a large amount of methanol (100 mL) and dried under vacuum to give a powder.

Yield: 224 mg (36%). ^{1}H nuclear magnetic resonance (NMR) (300 MHz, $CDCl_3$): δ (ppm) 7.89 (Ar-*H*, d, $J = 8.4$, 6H), 7.68 (Ar-*H*, d, $J = 7.2$, 6H), 7.39–7.49 (vinylene-*H*, m, 12H), and 7.23 (Ar-*H*, d, $J = 9.0$, 6H). ^{13}C NMR (75.45 MHz, $CDCl_3$): δ (ppm) 147.9, 141.0, 134.6, 130.93, 130.89, 129.4, 129.1, 125.9, 124.4, 118.3, and 109.9. High resolution mass spectrometry (electrospray ionization) *m/z*: calcd. for $C_{45}H_{30}N_4$ $[M+H]^+$, 627.25; found, 627.2546.

Synthesis of network polymers

Sodium methoxide in methanol (1 M, 5 mL) was added to a mixture of phenylenediacetonitrile (234 mg, 1.5 mmol) and tris(*p*-formylphenyl)amine (329 mg, 1.0 mmol) in tetrahydrofuran (THF) (10 mL), and the solution was stirred for 10 min at room temperature under air. The reacted mixture was diluted with THF (10 mL) and then filtered to remove a solid. The solid was washed with THF (10 mL) and a large amount of methanol (100 mL) and dried under vacuum to give a powder. **pNWP**: 503 mg. **mNWP**: 478 mg. **oNWP**: 7 mg.

Measurements

Liquid-state ^{1}H and ^{13}C NMR spectra of molecule **3** were recorded on a JEOL EX-300 spectrometer. The mass analysis was performed by liquid chromatography–mass spectrometry–ion trap–time-of-flight (Shimadzu). The solid-state ^{1}H cross-polarization magic-angle spinning (CP/MAS) NMR spectrum was measured using a Varian NMR systems 400WB spectrometer with an MAS rate of 17 kHz using a 3.2 mmf rotor. A ^{1}H 90° pulse of 1.8 μs and a TPPM ^{1}H decoupling power of 102 kHz were used. The CP was achieved with radio-frequency powers of 62.5 kHz for ^{1}H and 80 kHz for ^{13}C. The CP contact time was 1 ms. The specific surface areas of the samples were measured by N_2 gas adsorption at 77 K using an automated adsorption apparatus (BELSORP-max, BEL Japan Inc.). The system and sample were outgassed at 293 K for 6 h to obtain a residual pressure of $<10^{-4}$ Pa prior to the adsorption experiments. Fluorescence spectra were obtained on an Ocean Optics USB4000 fiber spectrometer with an LED light source (365 nm). The absolute quantum yields were obtained by a QS-QEM-KIT (OptoSirius) with an LLS-365 LED light source, general purpose integrating sphere (SC-10065-LHF), and USB4000 fiber spectrometer with a calibrated light source (HL-3P-INT-CAL).

Results and discussion

Synthesis of network polymers

Both the model compound and network polymers were synthesized by the Knoevenagel condensation. Model compound, **3**, was obtained by the condensation of tris(*p*-formylphenyl)amine, **1**, and phenylacetonitrile, **2a**, in ethanol in the presence of a strong base, NaOMe in a methanol solution (Scheme 1). The condensation of **1** with phenylenediacetonitrile, **2b-d**, in ethanol gave ethanol-insoluble materials, but these were soluble in common good solvents (halogenated, ether, and aromatic solvents). These results indicated that the targeted network polymers were not obtained. Instead, these were complex oligomer mixtures. Thus, to synthesize the insoluble network polymers, other solvents were used. The condensation in THF furnished insoluble polymers in all organic solvents. The polymers, *para*-linked network, **pNWP**, and *meta*-linked network, **mNWP**, were obtained in quantitative yields (Scheme 1). However, *ortho*-linked network, **oNWP**, was obtained in very low yield (< 1%). This result was proposed to arise from a steric effect of the reactive acetonitriles.

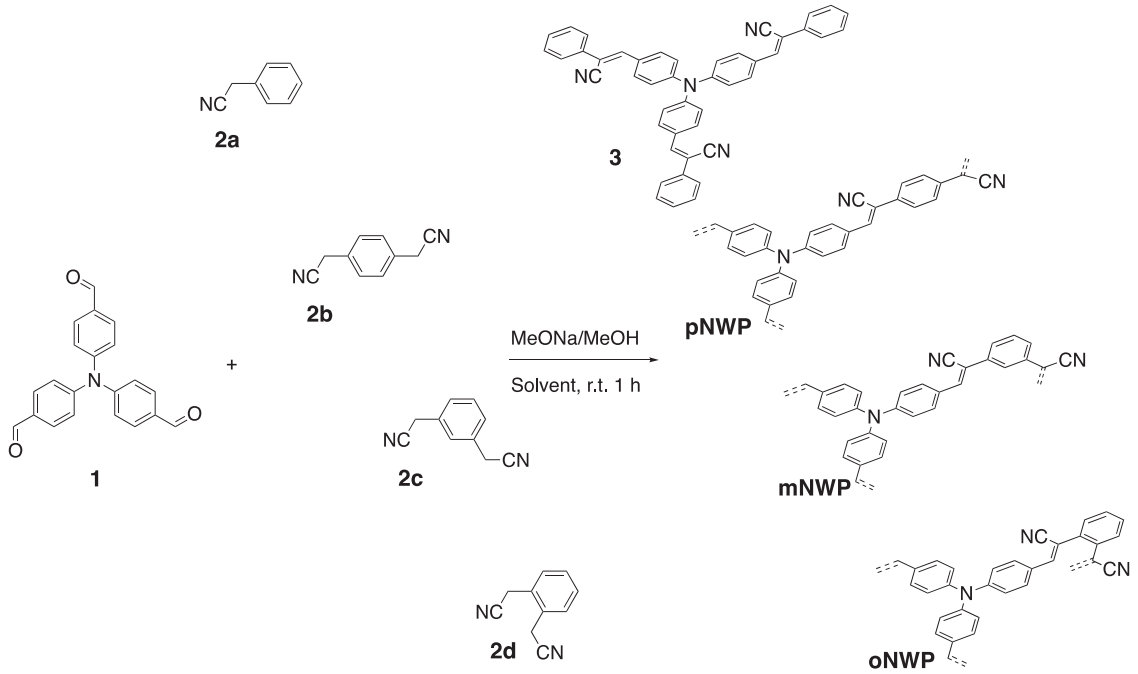

Scheme 1 Synthesis of the three-arm cyano-substituted phenylene-vinylene compound (**3**) and cyano-substituted phenylene-vinylene-based conjugated network polymers (**NWP**s) through the Knoevenagel condensation

Characterization of network polymers

The ^{1}H NMR spectrum of **3** is shown in Fig. S1A. The signals of the triphenylamine unit (***a*** and ***b***) of **3** were observed at 7.23 ppm (doublet) and 7.68 ppm (doublet). The signals of the cyano-substituted vinylene (***c***) and phenyl units (***d*** and ***e***) of **3** were observed at 7.89 (doublet) and 7.39–7.49 ppm, respectively. However, the ^{13}C NMR spectrum of **3** showed 11 signals in the aromatic region that were completely assigned to the carbons of **3** (Fig. S1B). The formation of cyano-substituted vinylene was confirmed by the observation of signal ***f***. Because the obtained materials **pNWP**, **mNWP**, and **oNWP** were insoluble, solid-state ^{13}C CP/MAS NMR was performed to investigate these network polymer structures. The ^{13}C CP/MAS NMR spectra of **pNWP**, **mNWP**, and **oNWP** are shown in Fig. S1C–E with assignments of the respective resonances. The characteristic resonance peaks of these materials were mainly observed in the aromatic region. Peaks assigned to the triphenylamine unit (***a***, ***b*** and ***c***+***d***) were observed from 120 to 160 ppm with overlapped carbon peaks of ***e***, ***g***, ***h***, and ***i***. The aldehyde group carbon of triphenylamine appeared at 190 ppm when the Knoevenagel condensation was incomplete. The signal was not observed in the spectra of **pNWP** and **mNWP**, which indicated that the Knoevenagel condensation proceeded to completion for monomer **1**. However, a small signal was observed for **oNWP** (***k***): this peak was not the spinning-side band (SSB) because the SSB does not appear in the sweep range at 17 kHz MAS. The signal derived from the cyano-substituted vinylene moiety (***f***) of **pNWP** and **mNWP** was separately observed at 109 ppm (Fig. S1C, D), while such a signal was not observed in the spectrum of **oNWP** (Fig. S1E) because the signal ***f*** overlapped with other signals. A sharp signal at 31 ppm (***l***) was not attributed to the aromatic units of **oNWP** but was assigned to the unreacted methylene of the phenylacetonitrile: the unreacted acetonitrile of the end group.

The porosity of the insoluble materials was revealed by N_2 sorption isotherm measurements at 77 K (Fig. S3A, Table S1). The sorption profiles for **pNWP** and **mNWP** exhibited an apparent uptake at relatively low pressure ($P/P_0 < 0.1$), which demonstrated the microporous characteristic of the networks. The nitrogen adsorption increased with the relative pressure without a plateau, even when the relative pressure reached 1.0. This adsorption behavior suggested the existence of macropores. However, **oNWP** did not show such a profile owing to the lack of porous structures in **oNWP**. For **pNWP** and **mNWP**, the Brunauer–Emmett–Teller (BET) surface areas were evaluated to be 520 and 307 $m^2 g^{-1}$ and the total volumes were 0.008 and 0.014 $cm^3 g^{-1}$ (the micropore volumes calculated from the nitrogen isotherm at $P/P_0 = 0.10$ are 0.13 and 0.22 $cm^3 g^{-1}$). The *para*-linked network material (**pNWP**) exhibited a higher surface area than that of the *meta*-linked network material (**mNWP**). Such a difference was probably because the network structure was more rigid and homogeneous than the twisted meta-linked network. The pore size distribution calculated by the nonlocalized density

functional theory method showed that there were mainly micropores (Fig. S3C). To estimate the contribution of the microporosity to the total porosity of the network, we calculated the ratio of V_{micro}/V_{total} (Table S1). The BET surface area and pore size distribution could be controlled by the geometric design. Consequently, these structures will contribute to the response (chromic effect) of chemicals.

Optical properties

The ultraviolet–visible absorption spectra of **3** in various solvents are displayed in Fig. S4. Because the compound was composed of an electron-donor triphenylamine unit and an electron-acceptor cyano-substituted phenylene-vinylene moiety, the absorption spectrum of **3** in chloroform (orange line) showed absorption bands that were attributed to the π–π* transition (305 nm) and an intramolecular charge transfer (CT) transition (425 nm). However, the absorption spectrum of **3** as a solid (black line) showed a lower CT band (450 nm) derived from the intermolecular interaction. To estimate the contribution of the dielectric constant to the absorption band (solvatochromic shift), the spectra of **3** in hexane, toluene, chloroform, dichloromethane (DCM), acetone, ethanol, *N,N*-dimethylformamide (DMF), acetonitrile, and dimethyl sulfoxide (DMSO) were measured (Fig. S4). The spectra were slightly shifted to lower energy by increasing the dielectric constant, but the spectra in ethanol (green line) and acetonitrile (blue line) showed exceptional results. These results were of merit because the triphenylamine unit of **3** was somewhat susceptible to the external environment.

Fluorescence images of **3** under various conditions are displayed in Fig. 1a. The compound exhibited a yellow solid-state fluorescence. Interestingly, the compound showed solvatofluorochromism from bluish-green to yellow. The fluorescence spectra of **3** in various solvents provided the information on the solvatofluorochromism (Fig. 1b). The trend in the redshift of the fluorescence bands was in the order of the increasing dielectric constant of the solvents (Fig. 1c). This solvatochromic behavior is commonly known to occur in various donor–acceptor molecules. The quantum yields (Φ) of the solutions and the crystals were measured based on an absolute method using an integrating sphere equipped with a multichannel spectrometer. The Φ value of compound **3** in chloroform was 10%. However, the Φ value was increased in both lower and higher dielectric constant solvents compared with that in chloroform (Fig. 1c). This tendency was considered to be a consequence of the light emission efficiency being improved by suppressing the molecular vibration, probably because of the higher affinity for the donor–acceptor compound **3**.

Fluorescence spectra of **pNWP** and **mNWP** showed lower energy bands than that of **3** owing to an extension of the π-conjugated system (Fig. 2). The *p*-vinylene linkage between triarylamine and phenylene caused a fluorescence band with a maximum at 609 nm. However, **mNWP** showed a yellow fluorescence (peak: 565 nm) because of a *m*-vinylene linkage. Regioisomeric structures in the network π-conjugated polymers affected not only the adsorption properties but also the electronic system. The Φ value of **pNWP** (12%) was lower than that of **mNWP** (35%). These differences were probably due to the length of conjugation.

Solvent effect

To investigate the influence of organic molecules, we tested the doping of typical solvents in the network polymers. According to the results of **3**, the dielectric constant of the

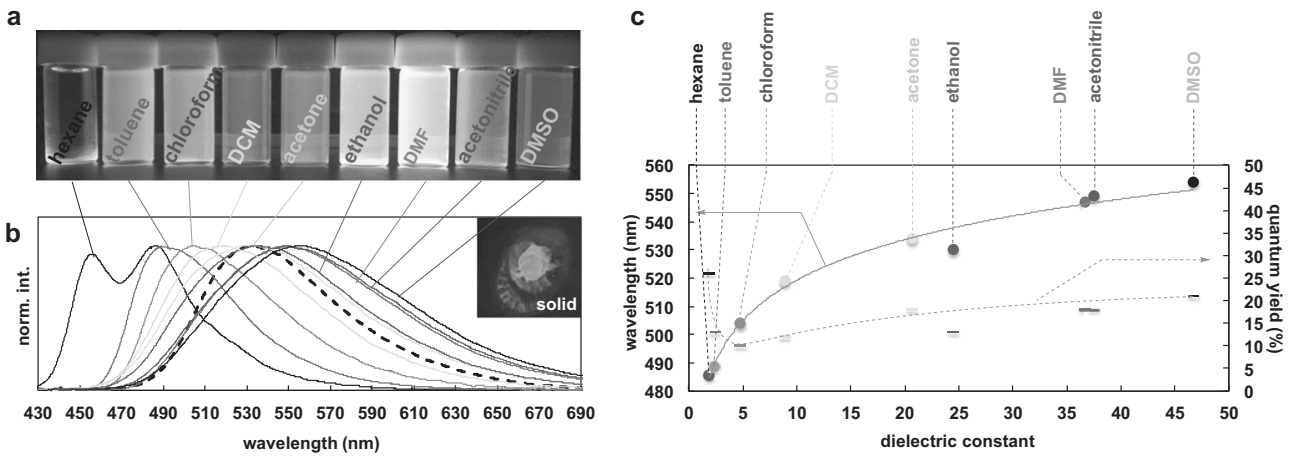

Fig. 1 **a** Images of **3** in various solvents under ultraviolet irradiation. **b** Photoluminescence spectra of **3** in various solvents. **c** Plots of the fluorescence maximum and quantum yield vs. the dielectric constant of the solvent

solvent effectively affected the band shift. However, the results of the network polymers were different from our estimation based on **3** (Fig. 3). The spectra of **pNWP** were changed in specific solvents that possessed a low dielectric constant (<7) (Fig. 3a). This characteristic phenomenon was ascribed to the swelling of **pNWP**. In this case, the good affinity of such solvents toward linear (*para*) π-conjugated structures would affect the excited state of **pNWP**. More surprisingly, **mNWP** also showed a characteristic changing of the fluorescence band, but this change was different from that of **pNWP**; **mNWP** in an aromatic solvent showed a redshifted band (Fig. 3b). These results probably arose from the difference in affinities of the network structure toward the solvents (Fig. 3c). Additionally, this phenomenon was also attributed to the swelling of **mNWP**. The porosity variations between **pNWP** (the *para*-structure) and **mNWP** (the *meta*-structure) probably caused the different affinities toward the solvents. In general, solubility depends on the rigidity of the conjugated structure, and the same dependence was also evident for the network polymers. We considered that the network polymer showed positive solvatochromism compared with the empty state by sensing solvent molecules within the network structure. The original spectrum returned upon drying, and a similar redshift was reobserved when we added the solvents again (Fig. S5).

The quantum yield also changed with the solvent addition. The Φ value of **pNWP** in polar solvents (ethanol, DMF, acetonitrile, and DMSO) was equal to that of the solid (12%), whereas in DCM and acetone, the Φ value was slightly increased (13%). However, **pNWP** in low-polarity solvents led to increases in Φ (hexane: 17%, toluene: 35%, anisole: 38%, chloroform: 37%, and chlorobenzene: 37%). However, the addition of nitrobenzene resulted in a reduction in the efficiency (<1%) due to quenching. The Φ value of **mNWP** in nonaromatic solvents (hexane, chloroform, DCM, acetone, ethanol, DMF, acetonitrile, and DMSO) was almost equal to that of the solid (34–37%). The addition of nitrobenzene also resulted in quenching (<1%). In other aromatic solvents, the Φ value was slightly increased (toluene: 45%, anisole: 39%, and chlorobenzene: 45%).

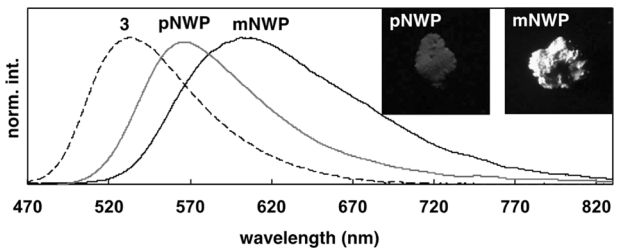

Fig. 2 Fluorescence spectra of **3**, **pNWP**, and **mNWP** in the solid state; the inset shows images of **pNWP** and **mNWP**

Summary

We have successfully demonstrated the facile synthesis of CMPs and their chemoselective response to work as a solvent sensor. The model small molecule based on triphenylamine and cyano-substituted vinylene showed a well-defined solvatofluorochromic response to the dielectric constant (ε_{sol}: ca. 0–50 vs. λ_{fl}: 480–560 nm). The response to solvents (chemicals) was also shown in the network polymers. The network polymer linked with *para*-phenylene-vinylene showed different solvatofluorochromic behaviors, namely, it was only responsive to the solvents with a low dielectric constant (ε_{sol} ca. <8) and nitrobenzene, which possesses a large ε_{sol} of approximately 35 and showed a

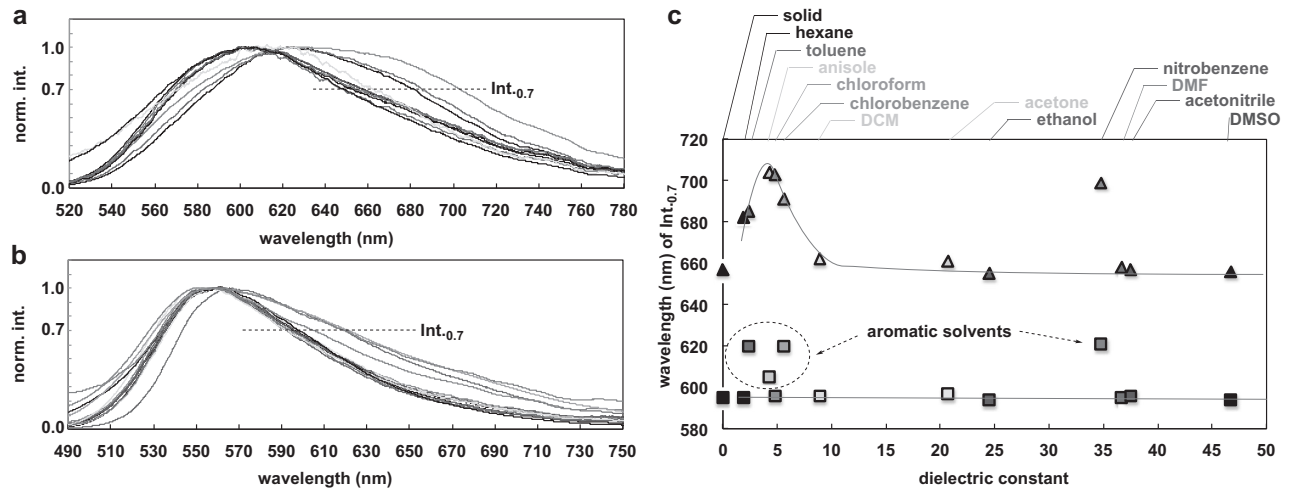

Fig. 3 **a** Photoluminescence spectra of **pNWP** in various solvents. **b** Photoluminescence spectra of **mNWP** in various solvents. **c** Plots of the wavelength of $Int_{0.7}$ vs. the dielectric constant of the solvent. The upper plot is obtained from **pNWP** and the lower obtained from **mNWP**. Wavelength of $Int._{0.7}$: 70% of the normalized intensity in the longer wavelength region

similar responsivity. More interestingly, the network polymer linked with *meta*-phenylene-vinylene was responsive to the aromatic solvents. Consequently, the characteristic chemoselectivity resulted from the geometric effect of the network structure. These network polymers will be used for chemical sensors.

Acknowledgements S.H. acknowledged a KAKENHI (Grant-in-Aid for Scientific Research B: no. 18H02052 and Grant-in Aid for Scientific Research in Innovative Areas "π-figuration": no. 17H05171) of the Japan Society for the Promotion of Science (JSPS). T.K. also acknowledged a KAKENHI (Grant-in-Aid for Scientific Research C: no. 17K05891) of JSPS. This work was performed under the Cooperative Research Program of the "Network Joint Research Center for Materials and Devices." We would like to thank Shimadzu for the HRMS measurements. We thank the Edanz Group (www.edanzediting.com/ac) for editing a draft of this manuscript.

Compliance with ethical standards

Conflict of interest The authors declare that they have no conflict of interest.

References

1. Jiang JX, Su F, Trewin A, Wood CD, Campbell NL, Niu H, et al. Conjugated microporous poly(aryleneethynylene) networks. Angew Chem Int Ed. 2007;46:8574–8.
2. Jiang J-X, Su F, Trewin A, Wood CD, Niu H, Jones JTA, et al. Synthetic control of the pore dimension and surface area in conjugated microporous polymer and copolymer networks. J Am Chem Soc. 2008;130:7710–20.
3. Dawson R, Laybourn A, Clowes R, Khimyak YZ, Adams DJ, Cooper AI. Functionalized conjugated microporous polymers. Macromolecules. 2009;42:8809–16.
4. Ben T, Ren H, Ma SQ, Cao DP, Lan JH, Jing XF, et al. Targeted synthesis of a porous aromatic framework with high stability and exceptionally high surface area. Angew Chem Int Ed. 2009;48:9457–60.
5. Yuan D, Lu W, Zhao D, Zhou H-C. Highly stable porous polymer networks with exceptionally high gas-uptake capacities. Adv Mater. 2011;23:3723–5.
6. Chen L, Yang Y, Jiang DL. CMPs as scaffolds for constructing porous catalytic frameworks: a built-in heterogeneous catalyst with high activity and selectivity based on nanoporous metalloporphyrin polymers. J Am Chem Soc. 2010;132:9138–43.
7. Jiang JX, Wang C, Laybourn A, Hasell T, Clowes R, Khimyak YZ, et al. Metal-organic conjugated microporous polymers. Angew Chem Int Ed. 2011;50:1072–5.
8. Xie ZG, Wang C, deKrafft KE, Lin WB. Highly stable and porous cross-linked polymers for efficient photocatalysis. J Am Chem Soc. 2011;133:2056–9.
9. Chen L, Honsho Y, Seki S, Jiang DL. Light-harvesting conjugated microporous polymers: rapid and highly efficient flow of light energy with a porous polyphenylene framework as antenna. J Am Chem Soc. 2010;132:6742–8.
10. Dawson R, Adams DJ, Cooper AI. Chemical tuning of CO_2 sorption in robust nanoporous organic polymers. Chem Sci. 2011;2:1173–7.
11. Li A, Sun HX, Tan DZ, Fan WJ, Wen SH, Qing XJ, et al. Superhydrophobic conjugated microporous polymers for separation and adsorption. Energy Environ Sci. 2011;4:2062–5.
12. Xu YH, Chen LZ, Guo Q, Nagai A, Jiang DL. Light-emitting conjugated polymers with microporous network architecture: interweaving scaffold promotes electronic conjugation, facilitates exciton migration, and improves luminescence. J Am Chem Soc. 2011;133:17622–5.
13. Liu X, Xu Y, Jiang D. Conjugated microporous polymers as molecular sensing devices: microporous architecture enables rapid response and enhances sensitivity in fluorescence-on and fluorescence-off sensing. J Am Chem Soc. 2012;134:8738–41.
14. Kou Y, Xu YH, Guo ZQ, Jiang DL. Supercapacitive energy storage and electric power supply using an aza-fused π-conjugated microporous framework. Angew Chem Int Ed. 2011;50:8753–7.
15. Ding S-Y, Wang W. Covalent organic frameworks (COFs): from design to applications. Chem Soc Rev. 2013;42:548–68.
16. Bhunia A, Dey S, Bous M, Zhang C, von Rybinski W, Janiak C. High adsorptive properties of covalent triazine-based frameworks (CTFs) for surfactants from aqueous solution. Chem Commun. 2015;51:484–6.
17. Kitagawa S, Kitaura R, Noro S. Functional porous coordination polymers. Angew Chem Int Ed. 2004;43:2334–75.
18. Sato H, Kosaka W, Matsuda R, Hori A, Hijikata Y, Belosludov RV, et al. Self-accelerating CO sorption in a soft nanoporous crystal. Science. 2014;343:167–70.
19. Blaker C, Pasel C, Luckas M, Dreisbach F, Bathen D. Investigation of load-dependent heat of adsorption of alkanes and alkenes on zeolites and activated carbon. Microporous Mesoporous Mater. 2017;241:1–10.
20. Kraus M, Trommler U, Holzer F, Kopinke F-D, Roland U. Competing adsorption of toluene and water on various zeolites. Chem Eur J. 2018;35:356–63.
21. Xu Y, Jin S, Xu H, Nagai A, Jiang D. Conjugated microporous polymers: design, synthesis and application. Chem Soc Rev. 2013;42:8012–31.
22. Xiang Z, Cao DJ. Porous covalent–organic materials: synthesis, clean energy application and design. J Mater Chem A. 2013;1:2691–718.
23. Dawson R, Cooper AI, Adams DJ. Nanoporous organic polymer networks. Prog Polym Sci. 2012;37:530–63.
24. Wang W, Zhou M, Yuan D. Carbon dioxide capture in amorphous porous organic polymers. J Mater Chem A. 2017;5:1334–47.
25. Li G, Qin L, Yao C, Xu Y. Controlled synthesis of conjugated polycarbazole polymers via structure tuning for gas storage and separation applications. Sci Rep. 2017;7:15394.
26. Xiao D, Li Y, Liu L, Wen B, Gu Z, Zhang C, et al. Two-photon fluorescent microporous bithiophene polymer via Suzuki cross-coupling. Chem Commun. 2012;48:9519–21.
27. Sun L, Liang Z, Yu J, Xu R. Luminescent microporous organic polymers containing the 1,3,5-tri(4-ethenylphenyl)benzene unit constructed by Heck coupling reaction. Polym Chem. 2013;4:1932–8.
28. Novotney JL, Dichtel WR. Conjugated porous polymers for TNT vapor detection. ACS Macro Lett. 2013;2:423–6.
29. Liu D-P, Chen Q, Zhao Y-C, Zhang L-M, Qi A-D, Han B-H. Fluorinated porous organic polymers via direct C–H arylation polycondensation. ACS Macro Lett. 2013;2:522–6.
30. Hayashi S, Togawa Y, Ashida J, Nishi K, Asano A, Koizumi T. Synthesis of π-conjugated porous polymers via direct arylation of fluoroarenes with three-arm triazine. Polymer. 2016;90:187–92.
31. Hayashi S, Togawa Y, Yamamoto S, Koizumi T, Nishi K, Asano A. Synthesis of π-conjugated network polymers based on fluoroarene and fluorescent units via direct arylation polycondensation

and their porosity and fluorescent properties. J Polym Sci Part A Polym Chem. 2017;55:3862–7.
32. Chi Z, Zhang X, Xu B, Zhou X, Ma C, Zhang Y, et al. Recent advances in organic mechanofluorochromic materials. Chem Soc Rev. 2012;41:3878–96.
33. Hayashi S, Hirai R, Yamamoto S, Koizumi T. A simple route to unsymmetric cyano-substituted oligo(p-phenylene-vinylene)s. Chem Lett. 2018;47:1003–5.
34. Hayashi S, Sakamoto M, Ishiwari F, Fukushima T, Yamamoto S, Koizumi T. A versatile scaffold for facile synthesis of fluorescent cyano-substituted stilbenes. Tetrahedron. 2019;75: 1079–84.
35. Wei Y, Chen W, Zhao X, Ding S, Han S, Chen L. Solid-state emissive cyanostilbene based conjugated microporous polymers via cost-effective Knoevenagel polycondensation. Polym Chem. 2016;7:3983–8.